Cited3 activates Mef2c to control muscle cell differentiation and survival

Gnanapackiam Sheela Devakanmalai, Hasan E. Zumrut and Ertuğrul M. Özbudak*

Department of Genetics, Albert Einstein College of Medicine, Bronx, New York, NY 10461, USA

*Author for correspondence (ertugrul.ozbudak@einstein.yu.edu)

Biology Open 2, 505–514
doi: 10.1242/bio.20132550
Received 18th July 2012
Accepted 25th March 2013

Summary

Vertebrate muscle development occurs through sequential differentiation of cells residing in somitic mesoderm – a process that is largely governed by transcriptional regulators. Our recent spatiotemporal microarray study in zebrafish has identified functionally uncharacterized transcriptional regulators that are expressed at the initial stages of myogenesis. *cited3* is one such novel gene encoding a transcriptional coactivator, which is expressed in the precursors of oxidative slow-twitch myofibers. Our experiments placed *cited3* into a gene regulatory network, where it acts downstream of Hedgehog signaling and *myoD/myf5* but upstream of *mef2c*. Knockdown of expression of *cited3* by antisense morpholino oligonucleotides impaired muscle cell differentiation and growth, caused muscle cell death and eventually led to total immotility. Transplantation experiments demonstrated that Cited3 cell-autonomously activates the expression of *mef2c* in slow myofibers, while it non-cell-autonomously regulates expression of structural genes in fast myofibers. Restoring expression of *cited3* or *mef2c* rescued all the *cited3* loss-of-function phenotypes. Protein truncation experiments revealed the functional necessity of C-terminally conserved domain of Cited3, which is known to mediate interactions of Cited-family proteins with histone acetylases. Our findings demonstrate that Cited3 is a critical transcriptional coactivator functioning during muscle differentiation and its absence leads to defects in terminal differentiation and survival of muscle cells.

Key words: Myogenesis, Muscle cell death, Zebrafish, mef2c, Cited, Differentiation

Introduction

Skeletal muscle is a major tissue type comprising around 40 percent of the adult mass, controlling locomotion and body-support, and accounting for most of an individual's daily energy consumption. Loss of skeletal muscle mass and/or strength occurs during aging, disease, or inactivity (Evans, 2010). When the function of the muscle tissue is impaired it results in various metabolism- and motility-related defects. One of the therapeutic avenues for treating muscle diseases is cell-based therapies, where functional muscle cells will be generated and amplified in culture, and finally delivered into patient tissue. However, generation of functional muscle cells requires a detailed understanding of how muscle cells differentiate in the first place.

As in other tissue types, specification of muscle cells does not rely on a linear regulatory pathway but rather on a network of interlinked signaling pathways and transcriptional regulators (Parker et al., 2003; Berkes and Tapscott, 2005; Ochi and Westerfield, 2007; Bryson-Richardson and Currie, 2008). Hence, elucidating this process can serve as a model for understanding development of other tissues. To identify the transcriptional regulators that are upregulated during the initial stages of muscle development *in vivo*, we microdissected zebrafish paraxial mesoderm into different spatiotemporal domains and performed microarrays (Ozbudak et al., 2010). Our recent study, for the first time, revealed the *in vivo* temporal induction order of transcriptional regulator genes as cells commit to muscle differentiation.

cited3, which is a member of the *CITED* (CBP/p300-interacting transactivator with glutamic acid/aspartic acid-rich tail) family transcriptional coactivator, was among the differentially expressed transcriptional regulators. Zebrafish *cited3* is orthologous with mammalian *Cited4*. Expression of *Cited4* was previously detected in human skeletal muscle tissue (Tews et al., 2007). Although the functional roles of *Cited* genes in skeletal muscle development have not been studied, they are important for mammalian development and have been implicated in cardiac (Sperling et al., 2005; Boström et al., 2010; MacDonald et al., 2012) and skeletal muscle (Pescatori et al., 2007; Sáenz et al., 2008; Tobimatsu et al., 2009) defects. *Cited2* RNA levels were significantly reduced in Duchenne muscular dystrophy and limb-girdle muscular dystrophy 2A human patients (Pescatori et al., 2007; Sáenz et al., 2008) and overexpression of *Cited2* counteracts glucocorticoid-induced muscle atrophy in C2C12 myotubes in cell culture (Tobimatsu et al., 2009). On the other hand, an increased level of Cited4 was previously associated with cardiomyocyte growth and proliferation in mice (Boström et al., 2010). Therefore, we decided to investigate the functional role of *cited3* in skeletal muscle development.

An elegant lineage-tracing study in zebrafish previously demonstrated that slow muscle cells differentiate from their

progenitor adaxial cells residing next to the midline axis in the somites (Devoto et al., 1996; Ochi and Westerfield, 2007; Stellabotte and Devoto, 2007; Bryson-Richardson and Currie, 2008). By in situ hybridization, we identified that *cited3* is expressed in the precursors of slow myofibers and this expression is depended on Hedgehog signaling via MyoD and Myf5.

We knocked down the expression of *cited3* by injecting two different antisense morpholino oligonucleotides that block splicing of *cited3*; this impaired muscle cell differentiation and growth, increased the number of apoptotic muscle cells and eventually led to total immotility. Overexpression of *cited3* mRNA rescued all the *cited3* loss-of-function phenotypes. In situ hybridization for various muscle-specific genes placed *cited3* into a gene regulatory network, where it acts downstream of *myoD/myf5* but upstream of *mef2c*. We identified that *mef2c* is the main target of Cited3 as its phenotype is rescued by restoring expression of *mef2c*. These data make a new and unprecedented connection between Cited3 and Mef2c – a crucial transcription factor for both heart and skeletal muscle tissues (Lin et al., 1997; Nakagawa et al., 2005; Hinits and Hughes, 2007; Potthoff et al., 2007; Potthoff and Olson, 2007). This is the first report demonstrating a Cited-family transcriptional coactivator functioning in the early stages of muscle development.

Materials and Methods

Zebrafish strains

Wild-type AB and TB fish strains were raised in the fish facility. Loss-of-function experiments of FGF signaling was performed using transgenic fish with heat-shock-driven expression of *dn-fgfr1* Tg (*hsp70: dn-fgfr1-gfp*) (Lee et al., 2005). Loss of function of Wnt signaling was accomplished by using transgenic fish with heat-shock-driven expression of *Δ*tcf: Tg (*hsp70: Δtcf-gfp*), (Lewis et al., 2004). Gain of function of Wnt signaling was performed by using transgenic fish with heat-shock driven expression of *wnt8:* Tg (*hsp70: wnt8-gfp*) (Weidinger et al., 2005). *myf5*^{hu2022} mutant were obtained from the Wellcome Trust Sanger Institute. Fish were bred and maintained at 28.5℃ on a 14–10 h light/dark cycle as described (Westerfield, 1993).

Microinjection

Capped RNA for microinjection was synthesized by *in vitro* transcription according to Manufacturer's protocol (Ambion, the RNA Company, Texas, US) from linearized plasmid of *pCS2*$^{+}$*-cited3*-254 (coding for full-length 254 amino acids), *pCS2*$^{+}$*-cited3-200* and *pCS2*$^{+}$*-Mef2c* (Mouse cDNA, kind gift from Stephen Tapscott). Antisense *cited3* (S1) morpholino oligonucleotide (MO) 'TCTCCC-TTCATTAAAACACACAAGA' and *cited3* (S2) MO 'GCATCATCATGTGC-TCTGCCATAGA', are synthesized to block the proper splicing of *cited3* at two different domains, were injected at a concentration of 0.8 or 12 ng/embryo, respectively, and both produced similar phenotypes. *myoD* MO 'ATATCCGACA-ACTCCATCTTTTTTG', was injected at 0.4 ng/embryo according to Hinits et al. (Hinits et al., 2009). Equivalent concentration of *control* MO (Gene Tools) was injected as a control. Fertilized eggs at one- to four-cell stages were microinjected with 80–200 pg RNA/embryo. Embryos were fixed at the desired stages in 4% paraformaldehyde fixative overnight at 4℃ and washed with phosphate-buffered saline and stored in methanol at −20℃ until use.

Gene cloning and in situ hybridization

The coding sequence of *cited3* was cloned into pDrive (Qiagen) and pCS2^{+} vectors by using cited3F: ATGGCAGAGCACATGATGATGCC and cited3R: TCAGCAGCTAACGGTGCTCGG primers. The C-terminally truncated *cited3* variant is created by placing a stop codon after the first 199th amino acids. Whole-mount in situ hybridization was carried out as previously described (Thisse and Thisse, 2008). Antisense RNA probes were synthesized by *in vitro* transcription from linearized plasmids using RNA polymerase T7 or T3 enzyme and digoxigenin RNA labeling mix (Roche). The following in situ hybridization probes were used: *myod, myf5* (cb641 from ZIRC), *mef2ca, prox1, stnnc* and *smyhc1* (kind gift from Phillip Ingham), *alpha actinin, myogenin, myhz1, myhz2, mylc2, tnnt1* and *tnnt3b* (kind gift from Monte Westerfield), *mef2d* (kind gift from Simon Hughes), *cmlc2* (kind gift from Deborah Yelon). Mouse *Mef2c* mRNA (kind gift from Stephen Tapscott) was injected in rescue experiments. Double fluorescent in situ hybridization was done following the protocol of Brend and Holley (Brend and Holley, 2009).

Immunostaining

The following primary antibodies were used: F59 IgG (1:10 dilution) mainly detects slow muscle specific myosin heavy chain, S58 (1:10 dilution) detects slow muscle specific myosin heavy chain, MF20 (1:10 dilution) labels all differentiated muscle fibers and F310 (1:10 dilution) labels fast muscle specific myosin heavy chain were obtained from DSHB. Anti-Mef2 (1:100 dilution) was obtained from Santa Cruz. The following secondary antibodies were used at 1:800 dilutions: Alexa Fluor 488 or 555 goat anti-mouse IgG1 or IgA, Alexa Fluor 568 or 647 goat anti-rabbit IgG, Alexa Fluor 647 goat anti-mouse IgG2b (Molecular Probes). Immunostaining was performed following the method of Bird et al. (Bird et al., 2012).

BrdU and Tunel staining

Embryos were pulsed for different time periods in 1 mM BrdU (Sigma), fixed in 4% PFA and stained using anti-BrdU antibody (Sigma) following the protocol of Barresi et al. (Barresi et al., 2001) with minor modification for whole mount and on sections. To identify apoptotic cells, in situ cell death detection kit (Roche) was used. Embryos fixed (4% PFA) at different stages were treated with Proteinase K 1 μg/ml according to the stage and washed with PBST and stained with TMR red for 30–60 minutes at 37℃.

Motility test

Embryos that are injected with *control* MO, *cited3 MO* or coinjected with *cited3 RNA* were tested for motility. Touch evoked response was recorded using live imaging of embryos from 2 days-post-fertilization (dpf) to 5 dpf using a Leica microscope and the speed of movements were analyzed using Sony Vegas movie Studio HD 9.0 software.

Imaging

In situ hybridized embryos and immunostained embryos were scanned under a Leica 205MA microscope and Carl Zeiss Imager Z2 equipped with apotome and axiovision 4.8 Rel. Serial sections of fluorescent images of antibody staining were taken at 1–3 μm intervals with Apotome and then 2D images were created by stacking all pictures taken at different focal planes.

Quantitation and statistical analysis

Mef2, Tunel and BrdU positive cells were counted using Image J. Cell counts were performed on z-stacks spanning an entire segment on one side of the embryo or on sections. Somites in 5–10 animals were scored and the experiments were reproduced minimum three times. Fluorescent images of different samples were taken on the same microscope with the same objective and exposure duration. The fluorescent intensity was quantified on the unmodified original images and the background intensity was subtracted by using Image J. F59 staining was diminished significantly after 2 dpf, while S58 staining was reduced at a slower pace and lost after 5 dpf. Therefore, we used S58 staining to count the number of slow fibers. Nevertheless, as S58 immunostaining was reduced in the morphants, we pseudo increased the intensity of staining in order to count the number of fibers. Fibers were counted on whole mount embryos on one hemi-segment in the anterior 10–12 somites and posterior 16–18 somites. Total number of fibers were counted from the 3D images acquired using axiovision software and verified with fluorescent intensity plots from plot profile using Image J (Barresi et al., 2001). All *P*-values were calculated by performing two-tailed Student's t-test in Excel. A *P*-value below 0.05 was considered statistically significant.

Cell transplantation

Cell transplantation was done following the protocol of Zeller and Granato et al. (Zeller and Granato, 1999). Donor embryos were injected with fixable tetramethyl rhodamine dextran fluorescent dye (Molecular Probes, D7162) with or without morpholinos. Cells from donor embryos were transplanted at shield stage into host embryos; chimeric embryos were identified, fixed, immunostained with F310 or F59 and Mef2 antibodies, and imaged.

Results

cited3 is expressed in the slow muscle precursors in somites and its expression is activated by Hedgehog signaling and *myod/myf5*

cited3 is expressed in the polster (arrow), which is the precursor of hatching gland, and in the notochord (red arrow) and chordo-neural hinge (green arrowhead) at 10 hpf (Fig. 1A). At 13 hpf, *cited3* is expressed in the slow muscle precursor adaxial cells (black arrowhead in Fig. 1B) on either side of the notochord. Subsequently, *cited3* transcripts become abundant in slow muscle

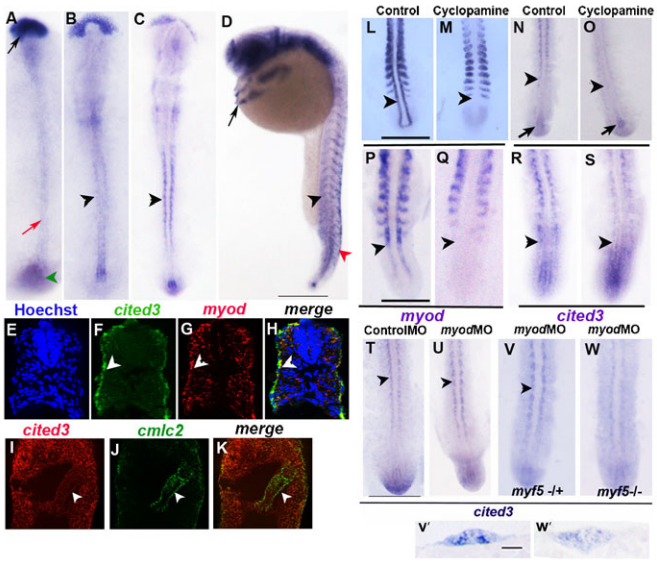

Fig. 1. Expression of *cited3* during segmentation stage. (**A**) *cited3* is expressed in the polster (black arrow) and in the notochord (red arrow) and chordo-neural hinge (green arrowhead) at 10 hpf. (**B**) At 13 hpf, *cited3* is expressed in the adaxial cells (slow muscle precursor; black arrowhead) on either side of the notochord. (**C**) Expression of *cited3* becomes abundant in the slow muscle precursors at 14 hpf. (**D**) *cited3* is also expressed in the differentiated slow muscle cells as indicated by black arrowhead and in the hatching gland as indicated by black arrow and neural crest cells (red arrowhead) at 24 hpf. (**E–H**) *cited3 is expressed in the differentiating slow muscle cells*. (E) Cross section of 24 hpf embryo depicting Hoechst staining in the nucleus; (F) *cited3* expression in the slow muscle domain; (G) *myod* expression in the slow and fast muscle domain; (H) merge of *cited3* and *myod* expression in the slow muscle domain (indicated by a white arrowhead). (**I–K**) *cited3 is expressed in the heart precursors.* (I) *cited3 is expressed* in the heart precursors both in the atrium and ventricle (J) *cmlc2* expression in the heart precursors (K) merge (ventral view of embryos). (**L–S**) *Expression of cited3 is regulated by the Hedgehog signaling* (L,N) Expression of *myoD, cited3* was not perturbed in ethanol treated control embryos, (M,O) but expression of *myod* and *cited3* is lost in the adaxial cells in cyclopamine treated (from 5–15hpf) embryos (indicated by arrowhead) whereas *myod* expression is still retained in the fast muscle (M) and *cited3* expression in the chordo-neural-hinge (arrow) (O). In comparison to control ethanol treatment, cyclopamine treatment from 13 to 18 hpf blocked transcription of *myod* in all adaxial cells (P,Q), but that of *cited3* only in adaxial cells located in the presomitic mesoderm (R,S). (**T–W**) *Myod and Myf5 redundantly regulate the expression of cited3.* (U) Expression of *cited3* was not perturbed in the embryos that were injected with *myoD* MO compared to those injected with the *control* MO (T) at 17 hpf. Similarly, expression of *cited3* was not affected in 75% of the embryos that were obtained from mating of heterozygous *myf5*^{hu202} mutant fishes and injected with the *myod* MO (22/28) (V,**V′**). However, expression of *cited3* was reduced or lost in the remaining 25% of the embryos from the same clutch injected with *myod* MO (6/28) (W,**W′**), while the remaining expression of *cited3* is in the neural crest cells. Scale bars: 100 µm in D,L,P,T, and 50 µm in V′.

cells at 14 hpf to 18 hpf (Fig. 1C) when they are known to differentiate and migrate to the periphery. Expression of *cited3* is detected in the hatching gland (black arrow), neural crest cells (red arrowhead), brain and branchial arches at 24 hpf (Fig. 1D). We performed double fluorescent in situ hybridization for *cited3* and *myod* on the cross-sections of embryos that are at 24 hpf. At this stage, differentiating slow myofibers are located lateral to the differentiating fast myofibers. We demonstrated that *cited3* is expressed only in the slow myofibers, while *myod* is expressed in both myofiber types (Fig. 1E–H). Double fluorescent in situ hybridization also revealed that *cited3* is expressed both in the atrium and ventricle heart precursors (Fig. 1I–K) overlapping with *cmlc2* expression (Yelon et al., 1999).

In order to identify the signaling pathways regulating *cited3* expression, we blocked the hedgehog signaling by treating embryos with hedgehog inhibitor cyclopamine or with ethanol as a control from 5 hpf to 15 hpf. As a control, we checked the transcription of *myod*, which is known to be lost only in the adaxial region upon loss of Hedgehog signaling (Lewis et al., 1999; Osborn et al., 2011). Transcription of both *myod* and *cited3* was lost in cyclopamine treated embryos in the adaxial region (Fig. 1M,O) but *myod* transcription was retained in precursors of fast myofibers and that of *cited3* was retained in the chordo-neural hinge, compared to ethanol treated embryos respectively (Fig. 1L,N). These results indicate that *cited3* is activated in response to Hedgehog signaling only in slow muscle precursors. Then we blocked the activity of Hedgehog signaling for a shorter duration starting at 13 hpf (when transcription of *cited3* is already turned on in the adaxial cells) until 18 hpf. This resulted in loss of *myod* transcription in the adaxial cells throughout the axis (Fig. 1P,Q), while *cited3* transcription is reduced only in the posterior-most part (presomitic mesoderm) of the adaxial region but not in the somites (Fig. 1R,S). Incubation of embryos with cyclopamine only for 2 hours from 13 hpf to 15 hpf reduced the transcription levels of *myod* drastically but not that of *cited3* (data not shown). The results suggest that *myod* is a direct target of Hedgehog signaling, while *cited3* might be indirectly regulated by Hedgehog signaling.

Then we investigated the regulatory relationship between *cited3* and muscle-regulatory-factors *myod* and *myf5*. We knocked down the expression of *myod* with the *myod* MO (Hinits et al., 2009). Expression of *cited3* was not affected in the *myod* morphants (Fig. 1T,U). Similarly, we checked the expression of *cited3* in embryos from the mating of heterozygous *myf5*^{hu202} mutants and found that its expression was not affected (data not shown). MyoD and Myf5 often regulate their targets redundantly. To investigate this possibility, therefore, we knocked down the expression of *myod* in embryos from *myf5*^{hu202} heterozygous incross and observed that expression of *cited3* was not affected in 75% of the embryos (Fig. 1V,V′) but was lost in the remaining 25% of embryos (Fig. 1W,W′). Hence, these results demonstrate that Myod and Myf5 redundantly activate transcription of *cited3*. Furthermore, they also suggest that Hedgehog signaling might activate the expression of *cited3* via activating the expression of *myod* and *myf5* (Lewis et al., 1999; Osborn et al., 2011) in the adaxial cells.

As Wnt and Fgf signaling are known to regulate muscle development, we tested the effect of these signaling factors on the expression of *cited3*. We perturbed the activities of Wnt and Fgf signaling in a time-resolved fashion by applying a pulse of heat-shock to transgenic embryos, where heat shock-responsive *hsp70* promoter activates the expression of various transgenes (supplementary material Fig. S1). However, we found that neither Wnt nor Fgf signaling regulate transcription of *cited3* (supplementary material Fig. S1).

Transcriptional coactivator domain of Cited3 is necessary for its function

We performed loss-of-function experiments for *cited3* to investigate its functional role during development. We designed two splice-blocking morpholino oligonucleotides (MO) targeting the first intron-exon boundary (S1-MO and S2-MO) of *cited3*. As

a control, we used the standard *control* MO that does not target any zebrafish gene. Subsequently, we confirmed the efficacy of two *cited3* MOs by RT-PCR: injection of each *cited3* MO prevented the splicing of the first intron significantly, whereas it is efficiently spliced out in the embryos injected with the *control* MO (supplementary material Fig. S2).

Knockdown of *cited3* resulted in obvious morphological phenotypes compared to wild-type embryos or embryos injected with the *control* MO starting after 1 dpf. In the *cited3* morphants, the heart was dilated, the body axis did not grow as much as it should (Fig. 2A,B), and the myosin heavy chain staining that is detected with F59 was reduced (Fig. 2E,F,I,J).

The specificity of the phenotype was verified by coinjection of full-length spliced mRNA of *cited3* along with *cited3* MOs. Full-length *cited3* mRNA rescued the *cited3* morphant phenotype (Fig. 2C,G,K).

Cited proteins are transcriptional coactivators. They interact with histone acetylases with their conserved C-terminal CR2 domain (Bragança et al., 2002). To assess whether the function of Cited3 protein depends on this conserved domain, we coinjected C-terminally truncated *cited3* mRNA with *cited3* MO. The truncated $cited3^{1-200}$ mRNA could not rescue the morphant phenotype; it also failed to rescue the F59 staining (Fig. 2D,H,L). Hence, we conclude that the transcriptional coactivator domain of Cited3 protein is necessary for its function during development.

Fig. 2M is the graphical representation of intensity measurements from F59 staining. Intensity of F59 staining was significantly reduced in *cited3* morphants when compared to that in wild-type (P-value$<2\times10^{-4}$); the staining was significantly rescued when the full-length *cited3* (P-value$<2\times10^{-2}$) but not the truncated $cited3^{1-200}$ RNA was co-injected (P-value>0.7). Interestingly, injection of full-length *cited3* RNA alone into wild-type embryos increased the myosin heavy chain expression significantly compared to that in wild-type embryos (data not shown).

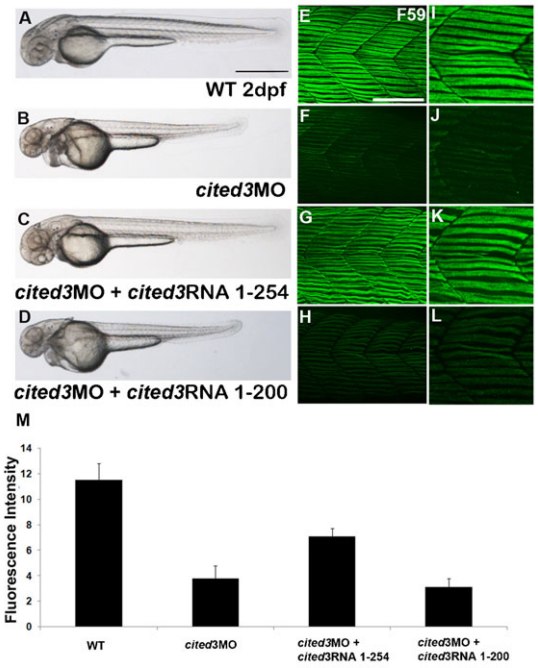

Fig. 2. Knock down of *cited3* disrupts muscle differentiation. (**A**,**B**) Knock down of *cited3* with two splice-blocking morpholino oligonucleotides (MO), S1-MO and S2-MO, resulted in thinner and shorter trunk, and dilated heart (B) compared to wild-type embryos (A) or embryos injected with the *control* MO (data not shown). Coinjection of full length *cited3* RNA (codes for 254 amino acid) rescued *cited3* morphant phenotype (**C**). (**D**) In contrast, coinjection of a C-terminally truncated form of *cited3* RNA (coding for the first 200 amino acids) did not rescue the morphant phenotype. (**E**) The expression of myosin heavy chain as evidenced by F59 antibody in an area covering somite 16^{th}–18^{th} in a wild-type embryo at 2 dpf. (**F**) The staining of F59 is reduced in embryos injected with *cited3* MO, whereas the expression of myosin heavy chain was restored when *cited3* RNA was co-injected with *cited3* MO (**G**) but not rescued when $cited3^{1-200}$ RNA was coinjected (**H**). (**I–L**) Magnified images of F59 staining. (**M**) The graphical representation of the average fluorescent intensity measurement of F59 immunostaining (of 10–18 embryos from three different experiments). Intensity of F59 staining was significantly reduced in *cited3* morphants when compared to that in wild-type (P-value$<2\times10^{-4}$), rescued when *cited3* RNA was co-injected (P-value$<2\times10^{-2}$) but not rescued when $cited3^{1-200}$ RNA was coinjected (P-value>0.7). Scale bars: 100 μm in A and 50 μm in E.

Cited3 stimulates the growth and maintenance of muscle fibers

Knockdown of *cited3* resulted in shorter embryos; this led us to test whether muscle cell growth is impaired and/or muscle cells are dying in the absence of *cited3*. First, we investigated muscle cell death in *cited3* morphants by using in situ cell death detection kit, TMR Red. These embryos were stained with anti-Mef2 antibody to identify muscle cells. *cited3* morphants had increased cell death in the muscle (Fig. 3D–F) compared to *control* MO injected embryos (Fig. 3A–C) and this phenotype was rescued in the embryos coinjected with *cited3* RNA (Fig. 3G–I). We quantified the number of apoptotic non-muscle versus muscle cells in all three treated groups. At 1 dpf, apoptotic cells were not found in the muscle of all three groups of embryos (data not shown). However, we found significantly higher number of apoptotic muscle cells in *cited3* morphants at 2 dpf and 3 dpf (Fig. 3M). Simultaneously, we did BrdU pulses in these embryos from 30 hpf to 42 hpf and 54 hpf to 66 hpf. We found that the numbers of BrdU positive cells were not significantly different in all the three treated groups (Fig. 3J–L; data not shown). Correlated with this finding, we still detect generation of thin secondary myofibers due to cell proliferation in *cited3* morphants after 1 dpf (data not shown). Hence, these results demonstrate that the absence of *cited3* leads to muscle cell apoptosis but it does not affect proliferation of the cells.

Next, we quantified the number of slow myofibers through 1–4 dpf by using slow muscle specific S58 antibody staining. *cited3* knockdown resulted in statistically significant reduction in the number of slow myofibers starting at 3 dpf, which was rescued by coinjecting *cited3* RNA (Fig. 4). *cited3* knockdown also prevented the growth of myofibers; the width and length of individual fibers and the width of somites were reduced significantly at 5 dpf (supplementary material Fig. S3). Correspondingly, the heights of somites were shorter in embryos that were injected with the *cited3* MO compared to those that were injected with the *control* MO (supplementary material Fig. S3). Altogether, these defects resulted in reduced motility in *cited3* morphants, which became totally immotile at 5 dpf as assessed by touch-evoked escape response test (supplementary material Fig. S4). The motility defect was significantly rescued by the coinjection of *cited3* RNA together with the *cited3* MO (supplementary material Fig. S4).

Cited3 regulates expression of *mef2ca* and *myogenin*

In order to identify where *cited3* fits in the gene regulatory network controlling muscle cell differentiation, we assessed

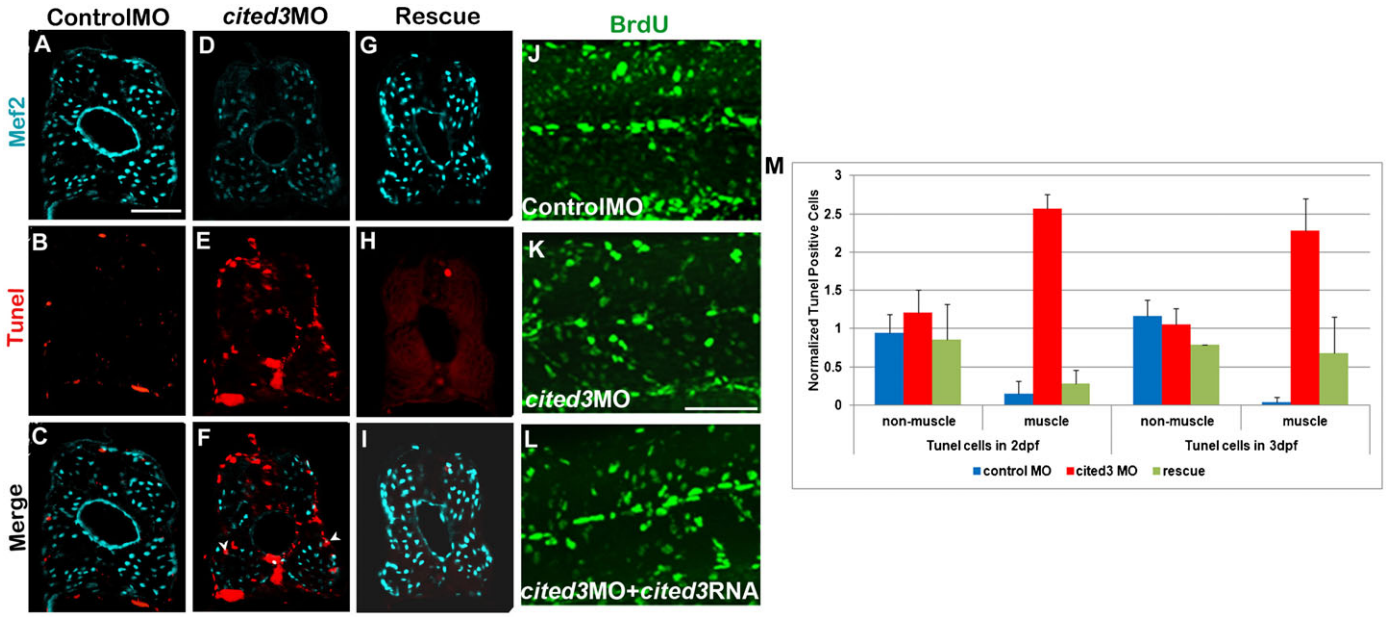

Fig. 3. Knockdown of *cited3* results in increased cell death but it does not affect proliferation. Embryos that are injected with the *control* MO (**A–C**), *cited3* MO (**D–F**), *cited3* MO + *cited3* RNA (**G–I**) were fixed at 2 dpf and immunostained with anti-Mef2 antibody (A,D,G) and TMR red in situ cell death detection kit (B,E,H). Tunel positive cells were counted in non-muscle cells as well as in muscle cells in each group of embryos from 50–100 sections obtained from trunk and tail somites. More apoptotic muscle cells were detected in embryos that are injected with the *cited3* MO and fixed at 2 dpf and 3 dpf (**M**). Values were normalized compared to *cited3* morphant values. Similarly, embryos injected with the *control* MO (**J**), *cited3*MO (**K**), *cited3* MO + *cited3* RNA (**L**) was pulsed with BrdU from 30 hpf to 42 hpf, and were fixed and immunostained with anti-BrdU and MF20 antibodies (images of 16^{th}–18^{th} somites). There is no significant difference between the three treated groups (J,K,L) when the BrdU-positive muscle cells were counted (data not shown). Scale bars: 25 µm in A and 50 µm in K.

expression levels of a set of muscle genes via in situ hybridization. We found that knockdown of *cited3* does not affect transcriptions of muscle regulatory genes *myod* (Fig. 5A,B) or *myf5* (Fig. 5C,D). But, differentiation marker *myogenin* transcripts were retained in *cited3* morphants at a stage when it is downregulated in control embryos (Fig. 5E,F). A similar effect on *myogenin* expression was previously detected when the expression of zebrafish *mef2* genes were lost (Hinits et al., 2009). Therefore, we checked the expressions of zebrafish *mef2* genes. Transcription of *mef2ca* was reduced in the *cited3* morphants compared to the *control* MO-injected embryos (Fig. 5G,H). Coinjection of *cited3* RNA along with *cited3* MO restored the *mef2ca* transcription (Fig. 5I). On the other hand, the transcription of *mef2d* was not perturbed (Fig. 5J–L).

We also validated our findings by immunostaining with the general Mef2 antibody that recognizes both Mef2c and Mef2d proteins in zebrafish (Hinits and Hughes, 2007). We found a significant reduction in the levels of total Mef2 proteins in *cited3* morphants and this was rescued by coinjection of *cited3* RNA (Fig. 5M–O). We also detected a similar phenotype in the heart, where Mef2 protein levels were reduced in heart cardiomyocytes of the *cited3* morphants. This phenotype was also rescued by coinjection of *cited3* RNA (Fig. 5M′–O′). Altogether, these results demonstrate that *cited3* functions upstream of *mef2ca* in the heart and skeletal muscle.

Cited3 cell-autonomously activates the expression of *mef2c* in slow muscle cells

In order to identify whether Cited3 activates the expression of *mef2c* cell-autonomously or not, we carried out cell transplantation experiments. As the anti-Mef2 antibody recognizes both Mef2c and Mef2d proteins and there are cell-to-cell variations in its staining, we quantified the intensity of Mef2 staining in both the transplanted and 8–10 closest neighboring slow myofibers that are located in the same somite. We transplanted presumptive slow muscle cells from donor wild-type embryos that are injected with the rhodamine dextran fluorescent dye into *control* MO injected host embryos of similar stage (Fig. 5P–R′). There was no significant difference in Mef2 protein levels between the transplanted wild-type slow myofiber and the slow myofibers in host embryos (Fig. 5Q; see supplementary material Fig. S5 for quantification). Similarly, we transplanted presumptive slow muscle cells from wild-type donors into *cited3* morphant hosts (Fig. 5S–U′) and found that Mef2 protein levels were retained in the wild-type transplanted cells that are surrounded by the morphant cells in which Mef2 protein levels were lower (Fig. 5T and quantified in Fig. 5Y). Whereas donor fibers that are transplanted from *cited3* MO injected embryos into wild-type hosts (Fig. 5V–X′) depicted a reduction in Mef2 protein levels (Fig. 5W and quantified in Fig. 5Z). Thus, these data demonstrate that *cited3* activates the expression of *mef2c* cell-autonomously in slow myofibers.

Expression of muscle structural genes are perturbed in *cited3* morphants

Expression levels of *prox1, smyhc1, alpha actinin, myhz1, myhz2 and mylc2* were not affected at 19 hpf (supplementary material Fig. S6). As differentiation proceeds further, transcription levels of *smyhc*, *stnnc*, *tnnt1*, *myhz2*, *mylc2*, *tnnt3b* and *myhz1* are declining in wild-type embryos at 2 dpf. However, their transcription levels were retained in *cited3* morphants at the same stage (Fig. 6A–N). Interestingly, fast-muscle specific F310 myosin heavy chain expression is reduced after 2 dpf in *cited3* morphants (Fig. 6P) compared to *control* MO injected embryos (Fig. 6O).

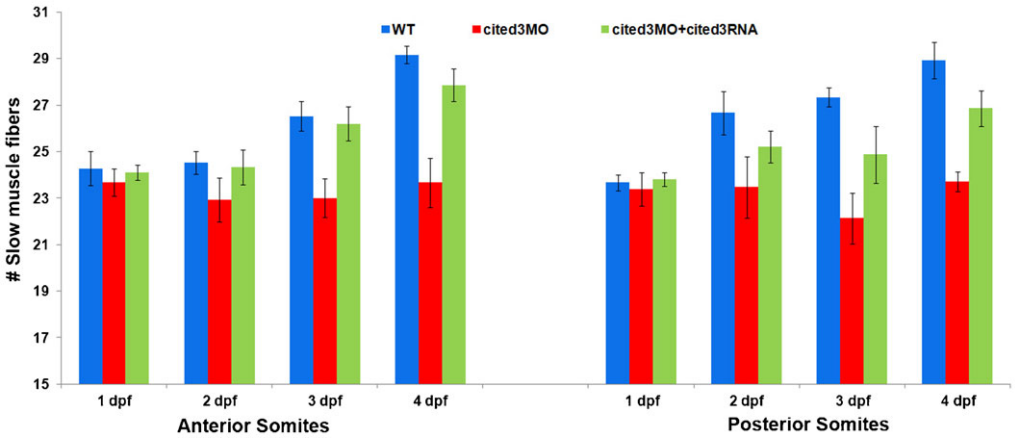

Fig. 4. The number of slow myofibers is reduced in *cited3* morphants starting at 3 dpf. The number of slow fibers was counted on whole mount embryos on one hemisegment from 10^{th}–12^{th} somites in the anterior region and 16^{th}–18^{th} somite in the posterior region of embryos at 1–4 dpf. Slow myofiber number is reduced significantly starting from 3 dpf in the morphant compared to WT (P-value$<2\times10^{-2}$ at 3 dpf and P-value$<2\times10^{-3}$ at 4 dpf) and was restored when *cited3*RNA was coinjected (P-value$<4\times10^{-2}$ at 3 dpf and P-value$<5\times10^{-3}$ at 4 dpf).

Cited3 non-cell-autonomously activates expression of fast-myofiber specific myosin heavy chain expression

We detected transcription of *cited3* only in the slow fiber cells both by regular and fluorescent in situ hybridization. However, starting after 2 dpf, we have detected disturbances in the expression of slow myofiber specific genes *smyhc*, *stnnc* and *tnnt1* (Fig. 6A–F), fast myofiber specific genes *myhz2*, *mylc2* and *tnnt3b* (Fig. 6G–L), and *myhz1* (which is expressed in both fiber types) (Fig. 6M,N). Expression of fast myosin heavy chain that is detected by F310 antibody staining is also reduced in *cited3* morphants at the same stage (Fig. 6O,P). In order to identify whether Cited3 regulates expression of fast-myofiber specific myosin heavy chain cell-autonomously or not, we transplanted presumptive muscle cells from donor wild-type embryos that are injected with rhodamine dextran fluorescent dye into host embryos of similar stage that are injected with the *cited3* MO and stained embryos with F310 at 2 dpf. The transplanted wild-type fast myofibers express F310 at low levels that are comparable to their neighboring morphant fast myofibers (supplementary material Table S1; Fig. S7). This result suggests that fast-fiber myosin heavy chain expression is non-cell-autonomously upregulated by *cited3*. We performed the opposite experiment by transplanting cells from *cited3* morphants into wild-type hosts. The transplanted morphant cells expressed fast myosin heavy chain at comparable levels to their neighboring wild-type fast myofibers. Altogether, this result suggests that Cited3 acts non-cell-autonomously to promote terminal differentiation of fast myofibers.

Restoring the expression of *mef2c* rescues the phenotypes of loss-of-function of *cited3*

To determine whether *mef2c* transcription factor is the main target of Cited3, we coinjected mouse *Mef2c* RNA together with *cited3* MO into embryos. We found that *Mef2c* rescues the morphological phenotypes of the *cited3* morphants (Fig. 7A–C). Similarly, *Mef2c* also rescued expression of myosin heavy chain as detected by F59 staining (Fig. 7D–F). Furthermore, restoring the expression of *Mef2c* also prevented the increased cell death phenotype that was observed upon knockdown of *cited3* as revealed by the tunel staining (Fig. 7G–O). Quantification of apoptotic muscle cells confirmed that *cited3* maintains the muscle cells by activating the expression of *mef2c* as *Mef2c* could rescue the cell-death phenotype of *cited3* morphants (Fig. 7P).

Discussion

cited3 is placed in a regulatory network downstream of *myod/myf5* and Hedgehog signaling but upstream of *mef2ca*

The muscle regulatory factors (MRFs) MyoD, Myf5, Myogenin and Mrf4 initiate myogenesis (Parker et al., 2003; Berkes and Tapscott, 2005; Hinits et al., 2009). Mef2 proteins are expressed during terminal differentiation of muscle cells (Black and Olson, 1998). Expression of *Mef2c* is activated by the MRFs both in mice and zebrafish (Wang et al., 2001; Hinits et al., 2009). Later on, Mef2 proteins interact with the MRFs to cooperatively activate late-stage muscle differentiation genes (Penn et al., 2004). *Mef2c* is required for heart looping morphogenesis and formation of the right ventricle in mice (Lin et al., 1997). *mef2c* gene is duplicated in zebrafish. Morpholino-mediated knockdown of *mef2ca* (Ghosh et al., 2009) or *mef2cb* (Lazic and Scott, 2011) are reported to result in pericardial edema or cell addition defects from the secondary-heart field, respectively. *mef2ca*$^{-/-}$; *mef2cb*$^{-/-}$ double mutants had reduced expression of sarcomeric genes in zebrafish heart (Hinits et al., 2012). Skeletal muscle-specific deletion of Mef2c in mice results in pups that were slightly smaller than the wild-type littermates and the mutant mice died within the first day after birth. At earlier stages of development, *Mef2c*-deficient myocytes differentiate and fuse normally; however, muscles gradually become disorganized at later stages (Potthoff et al., 2007). Double knockdown of *mef2ca* and *mef2d* did not affect the initial differentiation and fusion of myoblasts, however, the myoblasts failed to complete sarcomere assembly and double morphant fish larva also exhibit motility defects starting at 1 dpf (Hinits and Hughes, 2007). This phenotype exhibits similarities to the skeletal muscle specific loss of *Mef2c* in mice.

Here, we showed that expression of *cited3* is activated by MyoD/Myf5 and Hedgehog signaling (Fig. 1). As transcription of *myod* switches off much faster than that of *cited3* upon blockage of Hedgehog signaling, it is highly likely that Hedgehog signaling activates expression of *cited3* via activating *myod* and *myf5* (Lewis et al., 1999; Osborn et al., 2011). Although the short time interval between reductions of transcription levels of *myod* to that of *cited3* in cyclopamine treated embryos suggests that Myod (and Myf5) directly activates transcription of *cited3*, we do not have a proof of a direct regulation at the moment. In turn, Cited3 activates expression of *mef2ca* (Fig. 5G–I, Fig. 8), which results in retainment of *myog* transcription at 22 hpf as previously observed in zebrafish (Hinits and Hughes, 2007). This results in

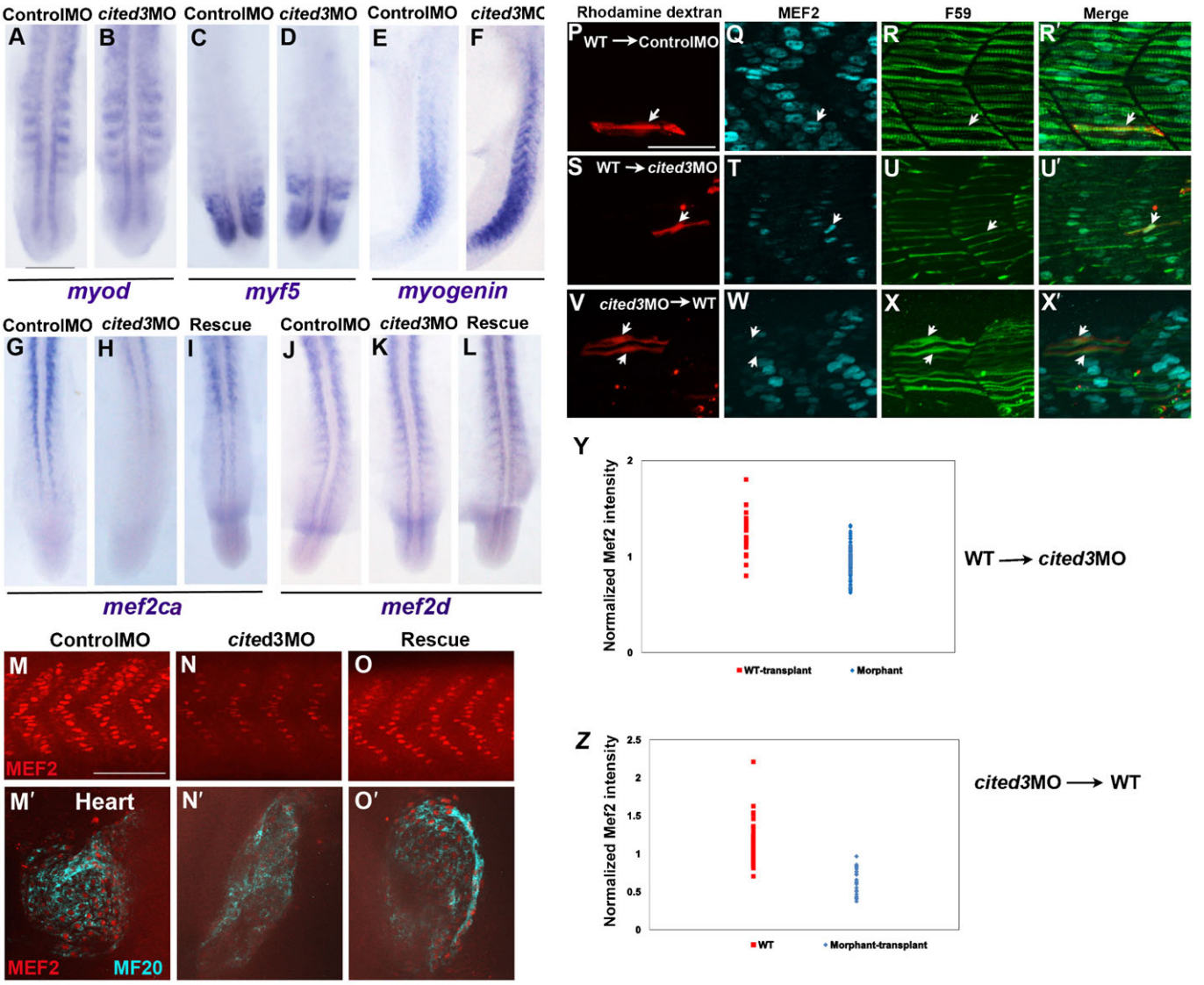

Fig. 5. Cited3 regulates expression of *mef2c* and *myogenin* and it acts cell-autonomously. (**A–D**) Expression of *myoD* and *myf5* was not perturbed in embryos injected with the *cited3* MO at 19 hpf. (**E**,**F**) *Myogenin* transcripts were retained in mature somites in the *cited3* morphants at 22 hpf (F) where it was usually downregulated in the *control* MO-injected embryos (E). Transcription of *mef2ca* was reduced in *cited3* morphants (**H**) compared to *control* MO-injected embryos (**G**) and it was restored to normal levels when coinjected with *cited3* RNA (**I**) at 19 hpf. (**J–L**) *Mef2d* expression was not affected in embryos injected with the *cited3* MO or *cited3* MO + *cited3* RNA at 19 hpf. (**M–O**) Immunostaining with the general anti-Mef2 antibody (recognizes all Mef2 variants) revealed that cumulative Mef2 protein levels were reduced in the *cited3* morphants (N compared to M) and were restored to normal levels when *cited3* RNA was coinjected (O) at 22 hpf (images spanning somites 16^{th}–18^{th} are shown) . Similarly, Mef2 protein levels were reduced in the heart of *cited3* morphants (**N′**) compared to the *control* MO-injected embryo (**M′**) and rescued in the *cited3* RNA coinjected embryos (**O′**) at 30 hpf. (**P–U′**) Slow muscle fibers labeled with rhodamine dextran dye were transplanted from wild-type donor embryos into *control* MO-injected (P–R′) or *cited3* MO-injected host embryos (S–U′). Anti-Mef2 immunostaining revealed that Mef2 protein levels in wild-type transplanted myofibers (arrowhead) were not different from those in the *control* MO injected host myofibers (Q), but were brighter compared to those in the *cited3* MO containing host slow myofibers (T). (**V–X′**) Mef2 staining in the transplanted *cited3* morphant myofibers is fainter than their wild-type host counterparts. (**Y**,**Z**) The normalized intensity of Mef2 protein level is plotted for different transplantation conditions. The number of quantified transplanted slow myofibers ranged from 23 to 141. *P*-values are 10^{-7} in Y and 10^{-12} in Z. Scale bars: 100 µm in A and 25 µm in M,P. Images in (P–U′) are from trunk somites, while those in (V–X′) are from anterior somites.

retainment of expression of muscle structural genes encoding various thin and thick filaments in myofibers at 2 dpf (Fig. 6).

mef2c is the main target of *cited3* both in the skeletal muscle and heart

Knockdown of *cited3* did not prevent initial differentiation and fusion of myoblasts at 1 dpf; it also did not perturb expression levels of various muscle structural genes at 19 hpf (supplementary material Fig. S6). However, *cited3* morphants failed to complete muscle differentiation, had muscle growth and maintenance defects and impaired motility (Figs 1–4; supplementary material Figs S3, S4). The onset of muscle differentiation and motility defects in the *cited3* morphants was at 2 dpf (Fig. 2; supplementary material Fig. S4), which is later compared to those in the double knockdown of *mef2ca* and *mef2d* (Hinits and Hughes, 2007). Likewise, expression levels of various muscle structural genes were perturbed at later stages (F59 staining at 30 hpf, F310 staining and transcription of other genes

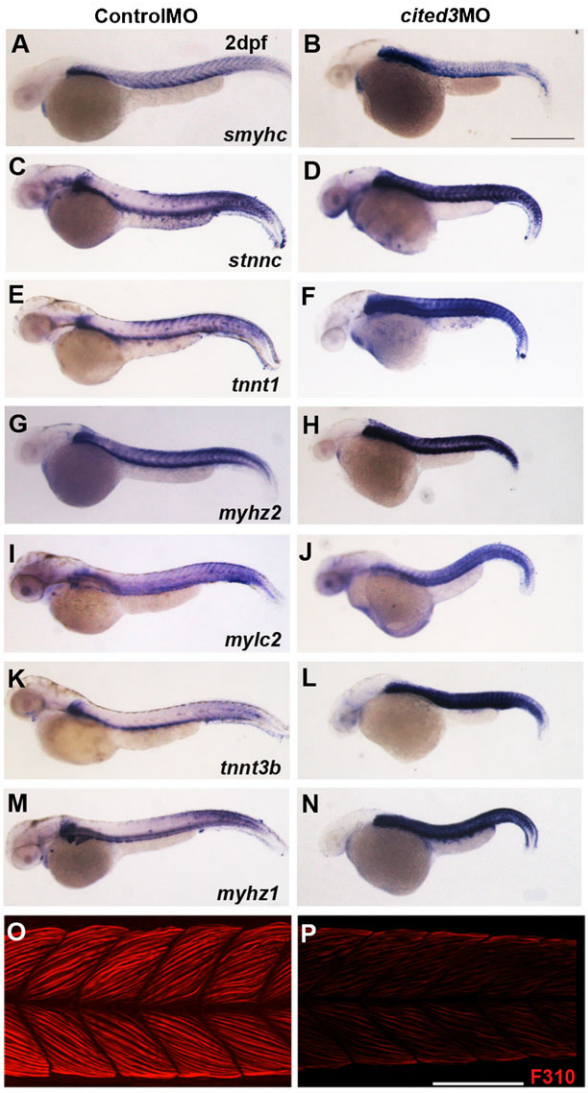

Fig. 6. Expression of various muscle structural genes were affected in cited3 morphants starting at 2 dpf. As differentiation proceeds, the expression levels of *smyhc*, *stnnc*, *tnnt1*, *myhz2*, *mylc2*, *tnnt3b* and *myhz1* in wild-type embryo were down regulated at 2 dpf (**A**,**C**,**E**,**G**,**I**,**K**,**M**). However, their respective expression in *cited3* morphants were retained (**B**,**D**,**F**,**H**,**J**,**L**,**N**). Expression of fast muscle myosin heavy chain is reduced after 2 dpf in *cited3* morphants (**P**) compared to *control* MO injected embryos (**O**) as evidenced by F310 immunostaining (somites 15^{th}–18^{th}). Scale bars: 100 µm in B and 25 µm in P.

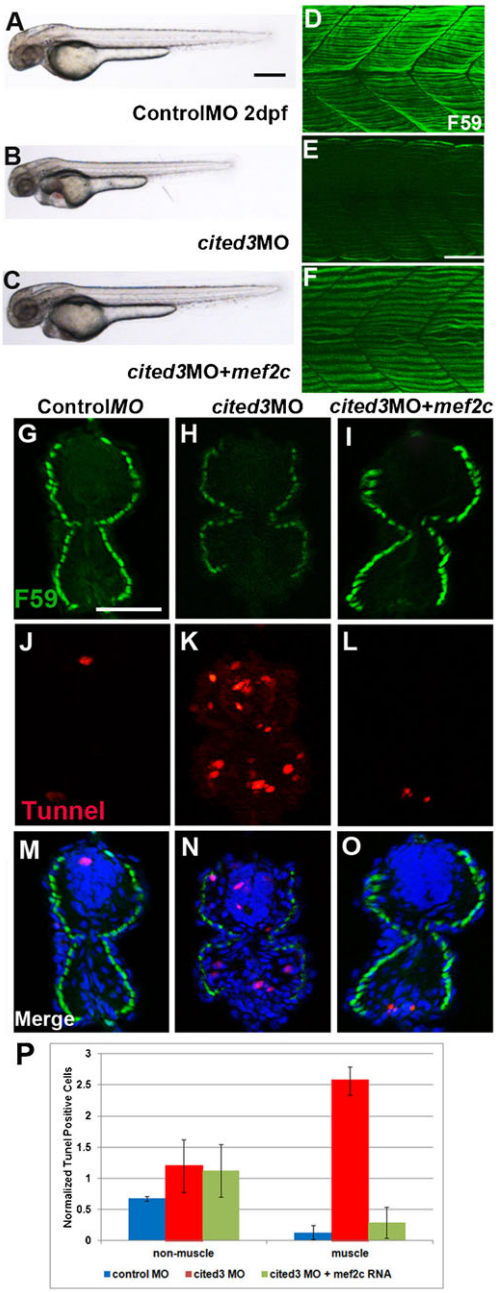

Fig. 7. Restoring expression of Mef2c rescues functional loss of *cited3* and prevents cell death. Coinjection of mouse *Mef2c* RNA rescues the morphological phenotypes (**A–C**) and the reduction in the expression of myosin heavy chain (15^{th}–18^{th} somites) (**D–F**) in the *cited3* MO-injected embryos. Coinjection of mouse *Mef2c* RNA also reduced the number of apoptotic muscle cells in *cited3* MO-injected embryos. (**H**,**K**,**N**) The number of apoptotic muscle cells are increased in *cited3* MO-injected embryos and it was restored to normal levels by the coinjection of mouse *Mef2c* RNA (as seen in **I**,**L**,**O**) as compared to *control* MO injected embryos (**G**,**J**,**M**). (**P**) Quantification of the apoptotic cells revealed that mouse *Mef2c* RNA significantly prevented the cell death in muscle cells of embryos that are coinjected with *cited3* MO. These are average values from 97 sections from trunk and tail of 5–10 embryos from three different experiments. Values were normalized compared to *cited3* morphant values. Scale bars: 100 µm in A and 25 µm in E,G.

at 2 dpf) in *cited3* morphants (Figs 2,6). This could be due to the persistence of *mef2d* transcripts in the *cited3* morphants (Fig. 5J–K). Strikingly, expression of mouse *Mef2c* rescued the *cited3* morphant phenotype (Fig. 7) suggesting that *mef2c* is the main transcriptional target of Cited3 in skeletal muscle differentiation. Interestingly, transcription of *mef2ca* starts at 14 hpf (Hinits and Hughes, 2007), which is soon after *cited3* is expressed in the adaxial cells (Fig. 1B) suggesting that *mef2ca* might be a direct target of Cited3.

Cited3 morphants also had a dilated heart. Due to its small size, fish embryos can develop and survive in the absence of a functional heart and blood circulation as oxygen is obtained via diffusion (Bakkers, 2011). Therefore, the skeletal muscle phenotype is unlikely to result from a defect in circulation. As *cited3* is expressed in the heart (Fig. 1) and regulates the levels of Mef2 proteins in the heart (Fig. 5), and mouse *Mef2c* rescues loss of function phenotype of *cited3* in the heart

(Fig. 7), *mef2c* is likely to be the major target of Cited3 also in the heart.

As *cited3* is functionally important for both heart and skeletal muscle development, Cited3 protein might interact with different tissue-specific transcription factors in each tissue or interact with the same transcription factor that is expressed in both tissues. At this point, we do not know which transcription factor Cited3 interacts with and also do not have a proof that Cited3 directly activates transcription of *mef2ca*. We will investigate these important questions and the detailed characterization of the heart phenotype in *cited3* morphants in our future studies.

cited3 non-cell-autonomously regulates differentiation and maintenance of fast myofibers

Although *cited3* is expressed only in the precursors of slow myofibers, loss of its expression also resulted in defects in fast myofibers. In addition to slow myofibers, apoptotic cells are also detected among fast myofibers after 2 dpf (Fig. 3). Expression levels of fast-fiber specific genes are also perturbed starting at 2 dpf (Fig. 6). Our cell transplantation experiments revealed that Cited3 activates expression of Mef2 proteins cell-autonomously in the slow myofibers (Fig. 5). However, expression of fast fiber specific myosin heavy chains (detected by F310) is non-cell-autonomously regulated by Cited3 (supplementary material Fig. S7; Table S1). Altogether, this result suggests that Cited3 acts non-cell-autonomously to promote terminal differentiation and maintenance of fast myofibers. Slow fibers are the first differentiating fiber type in zebrafish and their differentiation trigger timely differentiation of the progenitors of fast myofibers (Henry and Amacher, 2004). Our results suggest that slow myofibers play an instructive role in terminal differentiation of fast myofibers even after their initial migration (Henry and Amacher, 2004).

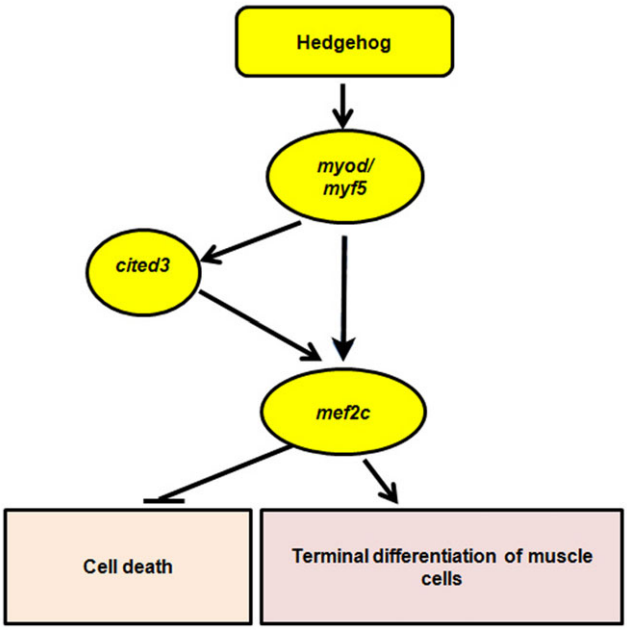

Fig. 8. Schematic representation of a genetic pathway that connects *cited3* to muscle cell differentiation and survival. Hedgehog signaling activated the expression of *myoD* and *myf5*, which in turn redundantly activates expression of *cited3* and *mef2c*. *cited3* in turn activates *mef2c*, which regulates muscle differentiation and prevents cell death. It is already known that *myoD* and *myf5* activates the expression of *mef2c*, which could be independent of the contribution of *cited3*.

This is the first report demonstrating the importance of the *cited3* gene in terminal muscle cell differentiation and maintenance

Muscle diseases develop due to genetic mutations, metabolic disorders and aging. Development of cellular therapies in which functional muscle cells are introduced into the patient muscles is one of the most promising avenues for treating muscle diseases. Recent progress in the efficiency of direct transdifferentiation of cells into a different cell fate (Davis et al., 1987; Takeuchi and Bruneau, 2009; Forsberg et al., 2010; Harvey, 2010; Ieda et al., 2010; Vierbuchen et al., 2010) demonstrated the importance of identifying gene clusters functioning during embryonic development of each tissue type. Discovering functionally significant genes in muscle development, likewise, has the potential to result in significant cell-based therapeutic advancement (Parker et al., 2003; Snider and Tapscott, 2003; Tajbakhsh, 2009). Strikingly, Mef2c, which we now have identified to be the target of Cited3, was previously demonstrated to cooperate with MyoD and Myogenin to enhance transdifferentiation of fibroblasts into muscle cells (Molkentin et al., 1995).

The functional roles of *Cited*-family genes in skeletal muscle development have so far not been investigated in any organism. However, expression of *Cited2* was reduced in Duchenne and limb-girdle muscular dystrophy patients (Pescatori et al., 2007; Sáenz et al., 2008). In contrast, overexpression of *Cited2* prevented drug-induced muscle atrophy in cell culture (Tobimatsu et al., 2009). Interestingly, loss of *Mef2* genes was also implicated in muscular atrophy in mammals (Yamakuchi et al., 2000; Uozumi et al., 2006; Tessier and Storey, 2010). This is the first report, where we demonstrate that expression of *cited3* is critical for muscle cell differentiation and maintenance and it acts through activating the expression of *mef2ca*.

Acknowledgements

We thank Dr Monte Westerfield, Simon Hughes, Stephen Devoto, Stephen Tapscott, Deborah Yelon and Phillip Ingham for plasmids; Bruce Appel (for the hsp70:gal4VP16), José Campos-Ortega (for the UAS: myc-notch1a-intra^kca3), Kenneth Poss (for the hsp70:dnfgfr1-EGFP), and Randall Moon (for the hsp70:wnt8a-GFP and hsp70l: ΔTcf-GFP) transgenic lines; Dr Stemple and the Wellcome Trust Sanger Institute for the myf5hu2022 mutant line. We also thank Burcu Guner-Ataman, Xin Li, Becky Weiss, Aaron Sarvet, Abdulvahap Sahin, Betul Sisman, Adem Demir, Rini Dcunha, Murat Isbilen, Cagri Kurt, Zeynep Ulupinar and Fatih Keles for technical help; Dr Florence Marlow for her support during the start-up phase of our lab; and members of Özbudak, Marlow and Jenny labs at the Albert Einstein College of Medicine for helpful discussions.

Competing Interests

The authors have no competing interests to declare.

References

Bakkers, J. (2011). Zebrafish as a model to study cardiac development and human cardiac disease. *Cardiovasc. Res.* **91**, 279-288.

Barresi, M. J., D'Angelo, J. A., Hernández, L. P. and Devoto, S. H. (2001). Distinct mechanisms regulate slow-muscle development. *Curr. Biol.* **11**, 1432-1438.

Berkes, C. A. and Tapscott, S. J. (2005). MyoD and the transcriptional control of myogenesis. *Semin. Cell Dev. Biol.* **16**, 585-595.

Bird, N. C., Windner, S. E. and Devoto, S. H. (2012). Immunocytochemistry to study myogenesis in zebrafish. *Methods Mol. Biol.* **798**, 153-169.
Black, B. L. and Olson, E. N. (1998). Transcriptional control of muscle development by myocyte enhancer factor-2 (MEF2) proteins. *Annu. Rev. Cell Dev. Biol.* **14**, 167-196.
Boström, P., Mann, N., Wu, J., Quintero, P. A., Plovie, E. R., Panáková, D., Gupta, R. K., Xiao, C., MacRae, C. A., Rosenzweig, A. et al. (2010). C/EBPβ controls exercise-induced cardiac growth and protects against pathological cardiac remodeling. *Cell* **143**, 1072-1083.
Bragança, J., Swingler, T., Marques, F. I. R., Jones, T., Eloranta, J. J., Hurst, H. C., Shioda, T. and Bhattacharya, S. (2002). Human CREB-binding protein/p300-interacting transactivator with ED-rich tail (CITED) 4, a new member of the CITED family, functions as a co-activator for transcription factor AP-2. *J. Biol. Chem.* **277**, 8559-8565.
Brend, T. and Holley, S. A. (2009). Zebrafish whole mount high-resolution double fluorescent in situ hybridization. *J. Vis. Exp.* **25**, e1229.
Bryson-Richardson, R. J. and Currie, P. D. (2008). The genetics of vertebrate myogenesis. *Nat. Rev. Genet.* **9**, 632-646.
Davis, R. L., Weintraub, H. and Lassar, A. B. (1987). Expression of a single transfected cDNA converts fibroblasts to myoblasts. *Cell* **51**, 987-1000.
Devoto, S. H., Melançon, E., Eisen, J. S. and Westerfield, M. (1996). Identification of separate slow and fast muscle precursor cells *in vivo*, prior to somite formation. *Development* **122**, 3371-3380.
Evans, W. J. (2010). Skeletal muscle loss: cachexia, sarcopenia, and inactivity. *Am. J. Clin. Nutr.* **91**, 1123S-1127S.
Forsberg, M., Carlén, M., Meletis, K., Yeung, M. S., Barnabé-Heider, F., Persson, M. A., Aarum, J. and Frisén, J. (2010). Efficient reprogramming of adult neural stem cells to monocytes by ectopic expression of a single gene. *Proc. Natl. Acad. Sci. USA* **107**, 14657-14661.
Ghosh, T. K., Song, F. F., Packham, E. A., Buxton, S., Robinson, T. E., Ronksley, J., Self, T., Bonser, A. J. and Brook, J. D. (2009). Physical interaction between TBX5 and MEF2C is required for early heart development. *Mol. Cell. Biol.* **29**, 2205-2218.
Harvey, R. P. (2010). Regenerative medicine: Heart redevelopment. *Nature* **467**, 39-40.
Henry, C. A. and Amacher, S. L. (2004). Zebrafish slow muscle cell migration induces a wave of fast muscle morphogenesis. *Dev. Cell* **7**, 917-923.
Hinits, Y. and Hughes, S. M. (2007). Mef2s are required for thick filament formation in nascent muscle fibres. *Development* **134**, 2511-2519.
Hinits, Y., Osborn, D. P. and Hughes, S. M. (2009). Differential requirements for myogenic regulatory factors distinguish medial and lateral somitic, cranial and fin muscle fibre populations. *Development* **136**, 403-414.
Hinits, Y., Pan, L., Walker, C., Dowd, J., Moens, C. B. and Hughes, S. M. (2012). Zebrafish Mef2ca and Mef2cb are essential for both first and second heart field cardiomyocyte differentiation. *Dev. Biol.* **369**, 199-210.
Ieda, M., Fu, J. D., Delgado-Olguin, P., Vedantham, V., Hayashi, Y., Bruneau, B. G. and Srivastava, D. (2010). Direct reprogramming of fibroblasts into functional cardiomyocytes by defined factors. *Cell* **142**, 375-386.
Lazic, S. and Scott, I. C. (2011). Mef2cb regulates late myocardial cell addition from a second heart field-like population of progenitors in zebrafish. *Dev. Biol.* **354**, 123-133.
Lee, Y., Grill, S., Sanchez, A., Murphy-Ryan, M. and Poss, K. D. (2005). Fgf signaling instructs position-dependent growth rate during zebrafish fin regeneration. *Development* **132**, 5173-5183.
Lewis, K. E., Currie, P. D., Roy, S., Schauerte, H., Haffter, P. and Ingham, P. W. (1999). Control of muscle cell-type specification in the zebrafish embryo by Hedgehog signalling. *Dev. Biol.* **216**, 469-480.
Lewis, J. L., Bonner, J., Modrell, M., Ragland, J. W., Moon, R. T., Dorsky, R. I. and Raible, D. W. (2004). Reiterated Wnt signaling during zebrafish neural crest development. *Development* **131**, 1299-1308.
Lin, Q., Schwarz, J., Bucana, C. and Olson, E. N. (1997). Control of mouse cardiac morphogenesis and myogenesis by transcription factor MEF2C. *Science* **276**, 1404-1407.
MacDonald, S. T., Bamforth, S. D., Bragança, J., Chen, C. M., Broadbent, C., Schneider, J. E., Schwartz, R. J. and Bhattacharya, S. (2012). A cell-autonomous role of Cited2 in controlling myocardial and coronary vascular development. *Eur. Heart J.* [Epub ahead of print].
Molkentin, J. D., Black, B. L., Martin, J. F. and Olson, E. N. (1995). Cooperative activation of muscle gene expression by MEF2 and myogenic bHLH proteins. *Cell* **83**, 1125-1136.
Nakagawa, O., Arnold, M., Nakagawa, M., Hamada, H., Shelton, J. M., Kusano, H., Harris, T. M., Childs, G., Campbell, K. P., Richardson, J. A. et al. (2005). Centronuclear myopathy in mice lacking a novel muscle-specific protein kinase transcriptionally regulated by MEF2. *Genes Dev.* **19**, 2066-2077.
Ochi, H. and Westerfield, M. (2007). Signaling networks that regulate muscle development: lessons from zebrafish. *Dev. Growth Differ.* **49**, 1-11.
Osborn, D. P. S., Li, K. Y., Hinits, Y. and Hughes, S. M. (2011). Cdkn1c drives muscle differentiation through a positive feedback loop with Myod. *Dev. Biol.* **350**, 464-475.
Ozbudak, E. M., Tassy, O. and Pourquié, O. (2010). Spatiotemporal compartmentalization of key physiological processes during muscle precursor differentiation. *Proc. Natl. Acad. Sci. USA* **107**, 4224-4229.
Parker, M. H., Seale, P. and Rudnicki, M. A. (2003). Looking back to the embryo: defining transcriptional networks in adult myogenesis. *Nat. Rev. Genet.* **4**, 497-507.
Penn, B. H., Bergstrom, D. A., Dilworth, F. J., Bengal, E. and Tapscott, S. J. (2004). A MyoD-generated feed-forward circuit temporally patterns gene expression during skeletal muscle differentiation. *Genes Dev.* **18**, 2348-2353.
Pescatori, M., Broccolini, A., Minetti, C., Bertini, E., Bruno, C., D'amico, A., Bernardini, C., Mirabella, M., Silvestri, G., Giglio, V. et al. (2007). Gene expression profiling in the early phases of DMD: a constant molecular signature characterizes DMD muscle from early postnatal life throughout disease progression. *FASEB J.* **21**, 1210-1226.
Potthoff, M. J. and Olson, E. N. (2007). MEF2: a central regulator of diverse developmental programs. *Development* **134**, 4131-4140.
Potthoff, M. J., Arnold, M. A., McAnally, J., Richardson, J. A., Bassel-Duby, R. and Olson, E. N. (2007). Regulation of skeletal muscle sarcomere integrity and postnatal muscle function by Mef2c. *Mol. Cell. Biol.* **27**, 8143-8151.
Sáenz, A., Azpitarte, M., Armañanzas, R., Leturcq, F., Alzualde, A., Inza, I., García-Bragado, F., De la Herran, G., Corcuera, J., Cabello, A. et al. (2008). Gene expression profiling in limb-girdle muscular dystrophy 2A. *PLoS ONE* **3**, e3750.
Snider, L. and Tapscott, S. J. (2003). Emerging parallels in the generation and regeneration of skeletal muscle. *Cell* **113**, 811-812.
Sperling, S., Grimm, C. H., Dunkel, I., Mebus, S., Sperling, H. P., Ebner, A., Galli, R., Lehrach, H., Fusch, C., Berger, F. et al. (2005). Identification and functional analysis of CITED2 mutations in patients with congenital heart defects. *Hum. Mutat.* **26**, 575-582.
Stellabotte, F. and Devoto, S. H. (2007). The teleost dermomyotome. *Dev. Dyn.* **236**, 2432-2443.
Tajbakhsh, S. (2009). Skeletal muscle stem cells in developmental versus regenerative myogenesis. *J. Intern. Med.* **266**, 372-389.
Takeuchi, J. K. and Bruneau, B. G. (2009). Directed transdifferentiation of mouse mesoderm to heart tissue by defined factors. *Nature* **459**, 708-711.
Tessier, S. N. and Storey, K. B. (2010). Expression of myocyte enhancer factor-2 and downstream genes in ground squirrel skeletal muscle during hibernation. *Mol. Cell. Biochem.* **344**, 151-162.
Tews, B., Roerig, P., Hartmann, C., Hahn, M., Felsberg, J., Blaschke, B., Sabel, M., Kunitz, A., Toedt, G., Neben, K. et al. (2007). Hypermethylation and transcriptional downregulation of the CITED4 gene at 1p34.2 in oligodendroglial tumours with allelic losses on 1p and 19q. *Oncogene* **26**, 5010-5016.
Thisse, C. and Thisse, B. (2008). High-resolution in situ hybridization to whole-mount zebrafish embryos. *Nat. Protoc.* **3**, 59-69.
Tobimatsu, K., Noguchi, T., Hosooka, T., Sakai, M., Inagaki, K., Matsuki, Y., Hiramatsu, R. and Kasuga, M. (2009). Overexpression of the transcriptional coregulator Cited2 protects against glucocorticoid-induced atrophy of C2C12 myotubes. *Biochem. Biophys. Res. Commun.* **378**, 399-403.
Uozumi, Y., Ito, T., Hoshino, Y., Mohri, T., Maeda, M., Takahashi, K., Fujio, Y. and Azuma, J. (2006). Myogenic differentiation induces taurine transporter in association with taurine-mediated cytoprotection in skeletal muscles. *Biochem. J.* **394**, 699-706.
Vierbuchen, T., Ostermeier, A., Pang, Z. P., Kokubu, Y., Südhof, T. C. and Wernig, M. (2010). Direct conversion of fibroblasts to functional neurons by defined factors. *Nature* **463**, 1035-1041.
Wang, D. Z., Valdez, M. R., McAnally, J., Richardson, J. and Olson, E. N. (2001). The Mef2c gene is a direct transcriptional target of myogenic bHLH and MEF2 proteins during skeletal muscle development. *Development* **128**, 4623-4633.
Weidinger, G., Thorpe, C. J., Wuennenberg-Stapleton, K., Ngai, J. and Moon, R. T. (2005). The Sp1-related transcription factors sp5 and sp5-like act downstream of Wnt/beta-catenin signaling in mesoderm and neuroectoderm patterning. *Curr. Biol.* **15**, 489-500.
Westerfield, M. (1993). *The Zebrafish Book: A Guide For The Laboratory Use Of Zebrafish (Brachydanio Rerio)*. Eugene, OR: M. Westerfield.
Yamakuchi, M., Higuchi, I., Masuda, S., Ohira, Y., Kubo, T., Kato, Y., Maruyama, I. and Kitajima, I. (2000). Type I muscle atrophy caused by microgravity-induced decrease of myocyte enhancer factor 2C (MEF2C) protein expression. *FEBS Lett.* **477**, 135-140.
Yelon, D., Horne, S. A. and Stainier, D. Y. R. (1999). Restricted expression of cardiac myosin genes reveals regulated aspects of heart tube assembly in zebrafish. *Dev. Biol.* **214**, 23-37.
Zeller, J. and Granato, M. (1999). The zebrafish diwanka gene controls an early step of motor growth cone migration. *Development* **126**, 3461-3472.